BMC Molecular and Cell Biology

RESEARCH

Open Access

Transient activation of YAP/TAZ confers resistance to morusin-induced apoptosis

Hoyeon Lee[1†], Sang Woo Cho[1†], Hyo Sun Cha[1], Kun Tae[1] and Cheol Yong Choi[1*]

Abstract

Background The Hippo signaling pathway involves a kinase cascade that controls phosphorylation of the effector proteins YAP and TAZ, leading to regulation of cell growth, tissue homeostasis, and apoptosis. Morusin, a compound extracted from *Morus alba*, has shown potential in cancer therapy by targeting multiple signaling pathways, including the PI3K/Akt/mTOR, JAK/STAT, MAPK/ERK, and apoptosis pathways. This study explores the effects of morusin on YAP activation and its implications for apoptosis resistance.

Results Our investigation revealed that morusin induces transient YAP activation, characterized by the dephosphorylation of YAP at S127 and nuclear localization, followed by gradual rephosphorylation in multiple cancer cells. Notably, this activation occurs independently of the canonical Hippo pathway and involves the LATS1/2, MINK1, and MAPK pathways during the YAP inactivation stage. Furthermore, morusin-induced stress granule formation was significantly impaired in YAP/TAZ-depleted cells, suggesting a role in apoptosis resistance. Additionally, the expression of constitutively active MINK1 maintained YAP activation and reduced apoptosis, indicating that prolonged YAP activation can enhance resistance to cell death.

Conclusions These findings suggest that YAP/TAZ are crucial in resistance to morusin-induced apoptosis, and targeting YAP/TAZ could enhance the anti-cancer efficacy of morusin. Our study provides new insights into the molecular mechanisms of morusin, highlighting potential therapeutic strategies against cancer by disrupting apoptosis resistance.

Keywords YAP/TAZ, Morusin, Stress granule, Apoptosis

Background

The Hippo signaling pathway is an evolutionarily conserved regulatory mechanism in biological processes such as cell proliferation, tissue homeostasis, organ size control, and apoptosis [1]. The Hippo pathway was originally discovered through genetic mosaic screens based on an overgrowth phenotype in mosaic flies, and has received significant attention because its dysregulation leads to a variety of diseases including cancer, hepatic diseases, and immune dysfunction [2–5]. The core components of the Hippo pathway are a kinase cascade involving the MST1/2 and LATS1/2 kinases, along with the associated regulatory proteins such as MOB1 and SAV1. This cascade ultimately modulates the activity of two primary effector proteins, Yes-associated protein (YAP) and transcriptional co-activator with PDZ-binding motif (TAZ). When the Hippo pathway is inactive, YAP and TAZ remain unphosphorylated and localize to the nucleus, where they activate target gene expression to

†Hoyeon Lee and Sang Woo Cho contributed equally to this work.

*Correspondence:
Cheol Yong Choi
choicy@skku.edu
[1]Department of Biological Sciences, Sungkyunkwan University, Suwon 16419, Republic of Korea

promote cell proliferation and survival. Conversely, when the Hippo pathway is activated, MST1/2 phosphorylates and activates LATS1/2, which in turn phosphorylates YAP and TAZ, leading to their cytoplasmic retention and subsequent degradation [6]. Dysregulation of this pathway, particularly through aberrant YAP/TAZ overexpression and mutations in upstream kinases, has been closely associated with the progression of various cancers [7, 8].

The functions of the core effectors YAP/TAZ are tightly regulated by post-translational modifications such as phosphorylation, ubiquitination, acetylation, and methylation [9]. Among these, the phosphorylation of YAP/TAZ primarily determines their stability, transcriptional activity, and subcellular localization. LATS1/2 protein kinases phosphorylate YAP at multiple sites, including serine 127 (S127) and serine 397 (S397), leading to cytoplasmic sequestration and subsequent degradation [10, 11]. In this phosphorylated state, YAP cannot interact with transcription factors such as TEAD, thereby inhibiting the expression of genes involved in cell growth, survival, and tissue homeostasis. Dephosphorylation of YAP at S127 results in release from 14-3-3 proteins and subsequent translocation to the nucleus, where it becomes active. Once in the nucleus, YAP can interact with various transcription factors, such as the TEAD family, SMAD family, RUNX family proteins, as well as β-catenin, to regulate gene expression. The function of YAP varies significantly depending on its binding partners, leading to diverse biological outcomes, ranging from promoting cell growth and survival to driving differentiation and apoptosis [12–15]. Thus, the dynamic regulation of YAP/TAZ by upstream kinases, including LATS1/2 and other protein kinases such as AMPK, the MAP4K family, and IKKβ/ε [16, 17], is critical for maintaining cellular equilibrium. Disruption of this regulation can result in uncontrolled cell proliferation and cancer [18–20]. Understanding the precise molecular mechanisms governing YAP/TAZ activity, including the dynamics of YAP phosphorylation and dephosphorylation, is essential for developing targeted cancer therapies.

YAP/TAZ, the main effectors of the Hippo pathway, directly or indirectly regulate several cancer hallmarks, including proliferation, survival, cancer stem cell maintenance, angiogenesis, metastasis, inflammation, and immunosuppression [1, 21]. These pathological conditions are often driven by mutations in upstream regulators or by the hyperactivation of YAP/TAZ due to enhanced nuclear localization. Hyperactivated YAP not only promotes tumor progression and metastasis but also contributes to an immunosuppressive environment. Active YAP induces the secretion of cytokines, such as CXCL5, which recruits CXCR2-expressing myeloid-derived suppressor cells (MDSCs) and type II macrophages [22]. This recruitment fosters an immunosuppressive tumor microenvironment, indirectly supporting tumor metastasis and enabling the tumor to evade immune attacks by T cells and NK cells. Furthermore, PD-L1, an immune checkpoint molecule, is a transcriptional target of Hippo signaling, further enhancing immune evasion [23]. Despite the low expression of YAP/TAZ in immune cells, the Hippo pathway plays a significant role in immune cell regulation. MST1/2 kinases are involved in $CD4^+$ T-cell proliferation and activation, lymphocyte adhesion, and macrophage homeostasis [24]. As a result, the tumor environment, shaped by recruited immune cells, secreted cytokines, and chemokines, is influenced by both non-canonical MST1/2 signaling and canonical YAP/TAZ activity. Together, these factors critically modulate immune responses within the tumor microenvironment. Beyond tumor progression and metastasis, YAP/TAZ dysfunction is implicated in inflammation-driven disorders affecting organs such as the heart, liver, lungs, intestines, and brain [25]. Inflammation is a vital defense mechanism after acute injury or in pathological conditions [26–28], and YAP/TAZ activation plays a key role in tissue regeneration following injury [22, 25]. YAP expression increases during tissue repair and regeneration, and its inactivation severely compromises this process [29]. Thus, while YAP/TAZ activation is essential for tissue remodeling and repair, these proteins represent promising therapeutic targets. Inhibiting their activity could potentially reprogram the tumor microenvironment to become more immune-permissive, offering new strategy for cancer treatment.

Morusin, a natural compound extracted from the plant *Morus alba*, is a phytochemical characterized by a prenyl group attached to a flavonoid backbone [30, 31]. It exhibits various pharmacological effects, demonstrating potential as a novel drug with anti-inflammatory [32], anti-cancer [33–37], antioxidant [38], and antibacterial properties [39]. Morusin has been reported to induce apoptosis in prostate cancer cells by inhibiting the STAT3 signaling pathway [33, 40] and to exert anti-cancer effects in renal cell carcinoma by suppressing the MAPK signaling pathway [37]. Additionally, it induces paraptosis-like cell death in epithelial ovarian cancer by causing mitochondrial calcium overload [36]. Morusin is also known to induce autophagy through ULK1 phosphorylation, leading to resistance to apoptosis [41], and to induce stress granule (SG) formation through PKR phosphorylation, thereby regulating the sequestration of the RACK1 pro-apoptotic protein [42]. Although accumulated evidence has shown the potential utility of morusin in targeting cancer cells, cancer cells often employ various evasion mechanisms, such as autophagy and SG formation, to resist morusin-induced cell death, necessitating further investigation into the underlying mechanisms.

In this study, we explored the impact of the Hippo pathway on the therapeutic potential of morusin-induced apoptosis in cancer cells. Our findings indicate that morusin triggers transient YAP activation and nuclear translocation, independent of the canonical Hippo pathway. This activation facilitates SG formation, providing a survival advantage to cancer cells under morusin-induced stress conditions. These insights could inform the development of novel cancer therapies that target YAP/TAZ and the associated pathways, thereby enhancing the efficacy of morusin as an anti-cancer agent.

Methods

Cell culture

HEK293A, HeLa, and HepG2 cells were cultured in Dulbecco's Modified Eagle's Medium (DMEM) supplemented with 10% fetal bovine serum (Gibco) and 1% penicillin-streptomycin solution. A549 and HCT116 cells were cultured in RPMI 1640 (Gibco) supplemented with 10% fetal bovine serum and 1% penicillin-streptomycin solution. HA-MINK1 overexpressing HCT116 cells were cultured in RPMI 1640 supplemented with 10% fetal bovine serum, 1% penicillin-streptomycin solution, and 1 μg/mL puromycin. The cells were maintained at 37 °C with 5% CO_2 and humidified air.

Antibodies and reagents

In this study, the following antibodies and reagents were used: Anti-pYAP (13008), anti-YAP (17074), anti-pLATS1 (8654), anti-LATS1 (3477), anti-pMST1/2 (49332), anti-MST1 (3682), anti-MST2 (3952), anti-pMOB1 (8699), anti-MOB1 (13730), anti-SAV1 (13301), anti-pJNK (9251), anti-JNK (9252), anti-LC3 (12741), anti-PARP (9542), anti-cleaved-caspase3 (9661), anti-laminB1 (12586) were purchased from Cell Signaling Technology. Anti-TAZ (GTX134857) was purchased from GeneTex. Anti-LATS2 (MBS7600942) was purchased from MyBioSource. Anti-YAP (sc-101199), anti-pERK (sc-7383), anti-ERK (sc-271269) were purchased from Santa Cruz Biotechnology. Anti-G3BP (611126) was purchased from BD Biosciences. Anti-p62 (ab56416) was purchased from Abcam. Anti-LC3 (PM036) was purchased from MBL Life Science. Anti-actin (A700-057), anti-GAPDH (A700-103) were purchased from Bethyl Laboratories. Anti-tubulin (05-829) was purchased from Merck Millipore. Anti-HA-HRP (12013819001) was purchased from Roche. Morusin (BP0961) was purchased from Chengdu Biopurify.

DNA and siRNA transfection

Human MAP4K6 was provided by the Korea Human Gene Bank, Medical Genomics Research Center, KRIBB, Korea. The gene was amplified by PCR and subcloned into the HA-tagged pLJC5 lentivirus expression plasmid. The constitutively active (CA) pLJC5 HA-MAP4K6 T187E was generated using the Muta-Direct™ Site Directed Mutagenesis Kit (iNtRON Biotechnology) following the manufacturer's protocol. The plasmids were transfected into HEK293T cells using Lipofectamine 3000 Transfection Reagent (Invitrogen) according to the manufacturer's protocol. Cells were reverse-transfected with siRNA using Lipofectamine™ RNAiMAX Transfection Reagent (Invitrogen) following the manufacturer's protocol. The following sequences of primers were used in this study: siYAP, 5'-GGUGAUACUAUCAACCAAAUU-3'; siTAZ, 5'-ACGUUGACUUAGGAACUUU-3'; siLATS1, 5'-GGUGAAGUCUGUCUAGCAA-3'; siLATS2, 5'-AAUCAGAUAUUCCUUGUUG-3'.

Establishment of cell lines overexpressing HA-MAP4K6

HEK 293T cells were transfected with lentivirus packaging plasmids, such as VSV-G and Gag-Pol, in combination with the pLJC5 HA-MAP4K6 WT or CA expression plasmid. The media was exchanged for complete media 8 h after transfection. After 48 h, the supernatant was harvested and filtered using a 0.45 μm syringe filter to collect the lentivirus particles. HCT116 cells were infected with the filtered lentivirus in complete media. The ratio of the mixture was 3:7, and 8 μg/mL of polybrene was added. After 12 h, the media was exchanged for complete media, and cells were selected with puromycin at 1 μg/mL after 24 h.

Immunoblotting

Cells were rinsed with ice-cold PBS and then lysed with ice-cold RIPA lysis buffer (1% NP-40, 0.1% SDS, 0.5% SDC, 150 mM NaCl, 50 mM Tris-Cl pH 8.0, 10 mM NaF, 5 mM, NEM, 1 mM Na_3VO_4, and Protease Inhibitor Cocktail (Sigma-Aldrich)). Lysates were incubated on ice for 30 min, and soluble fractions were separated by centrifugation at 13,500 rpm for 10 min. The supernatants were quantitated by the BCA assay and mixed with 5X Laemmli sample buffer. Next, the samples were boiled at 100 °C for 10 min. Samples were separated by size using SDS-PAGE, and proteins were transferred to PVDF membranes. The membranes were blocked with 4% skim milk for 30 min at room temperature, and incubated with primary antibodies overnight at 4 °C. Afterward, membranes were washed with TBST buffer 3 times for 10 min each at room temperature and then incubated with appropriate secondary antibodies for 1 h at room temperature. The membranes were washed with TBST buffer 3 times for 10 min each at room temperature, and results were detected using ECL substrate and Chemidoc. To determine the influence of ERK on YAP phosphorylation, HCT116 cells were pretreated with an MEK1 inhibitor (PD98059) to inhibit ERK1/2 activation, followed by treatment with either DMSO or morusin.

RNA isolation and qPCR

Cells were lysed with TRIzol reagent (Invitrogen) and total RNA was isolated using chloroform precipitation methods. 1 μg RNA was reverse transcribed and amplified to synthesize cDNA using Maxime™ RT-PCR PreMix (iNtRON Biotechnology) following the manufacturer's protocol. The synthesized cDNA was analyzed by quantitative real-time PCR using iQ™ SYBR Green Supermix (Bio-Rad). The following sequences of primers were used in this study: CTGF forward primer: 5′-CTTGCGAA GCTGACCTGGAAGA-3′; CTGF reverse primer: 5′-C CGTCGGTACATACTCCACAGA-3′; CYR61 forward primer: 5′-GGAAAAGGCAGCTCACTGAAGC-3′; CYR61 reverse primer: 5′-GGAGATACCAGTTCCACA GGTC-3′; GAPDH forward primer: 5′-GTCTCCTCTGA CTTCAACAGCG-3′; GAPDH reverse primer: 5′-ACCA CCCTGTTGCTGTAGCCAA-3′.

Immunofluorescence

Cells were cultured in 6-well plates on coverslips. The cells were rinsed with PBS and fixed with 3% paraformaldehyde for 15 min at room temperature. Afterward, the cells were washed once with PBS and permeabilized with 0.1% Triton X-100 in PBS for 5 min at room temperature. Subsequently, they were blocked with PBS containing 2% BSA for 20 min. Following blocking, cells were incubated with primary antibodies for 1 h at room temperature and then washed with PBS four times. Next, the cells were incubated with secondary antibodies and DAPI for 20 min at room temperature. The cells were washed with PBS four times and mounted in a 10% glycerol solution. Fluorescence was detected using a Zeiss LSM 700 confocal microscope and analyzed using ZEN software.

Nuclear/cytosol fractionation

Cells were lysed with Buffer A (10 mM HEPES, 1.5 mM $MgCl_2$, 10 mM KCl, 0.5 mM DTT, 0.05% NP40, pH 7.9) and incubated on ice for 10 min. To separate the cytosolic fractions of the cells, lysates were centrifuged at 3,000 rpm for 10 min, and the supernatants were transferred to new tubes. The pellets were resuspended in Buffer B (5 mM HEPES, 1.5 mM $MgCl_2$, 0.2 mM EDTA, 0.5 mM DTT, 300 mM NaCl, 26% glycerol, pH 7.9) and homogenized with 20 strokes on ice. Afterward, the lysates were incubated on ice for 30 min and centrifuged at 24,000 g for 20 min at 4 °C. The supernatants were transferred to new tubes, and all samples were quantitated by the BCA assay.

Cell viability analysis

Cell viability was assessed using the MTT (3-(4,5-dimethylthiazol-2-yl)-2,5-diphenyltetrazolium bromide) assay. Briefly, cells (1×10^3 cells/well) were seeded into 96-well plates and treated with morusin for 4 h. The viability of cells, indicated by MTT dye uptake, was determined by measuring the optical density at 570 nm using an enzyme-linked immunosorbent assay (ELISA) reader. The Cell Viability Assay Kit (Cat. No.11465007001, Roche Diagnostics) was utilized, and the procedure was performed according to the manufacturer's recommendations. Each experiment was repeated three times, and data are presented as the mean of triplicate wells ± SEM.

Statistical analysis

Statistical significance was performed by one-way analysis of variance (ANOVA) followed by Bonferroni's multiple comparison test with GraphPad Prism 5 software. P values < 0.05 were considered statistically significant.

Results

Morusin induces YAP activation

Morusin is known to induce cell death by inhibiting STAT3 activity [33] and modulating the PI3K/Akt, JNK, and ERK pathways [35]. However, cancer cells can resist this effect through evasion strategies such as autophagy and stress granule formation [41, 42]. The Hippo signaling pathway, which regulates cellular proliferation and differentiation, is also implicated in apoptosis resistance [43]. We hypothesized that the Hippo pathway might play a protective role against morusin-induced cell death by modulating YAP activation. To test this hypothesis, we treated various cancer cell lines with increasing concentrations of morusin for 3 h. We observed that morusin induces the dephosphorylation of YAP at S127, a site critical for its inhibitory function and protein stability, in a dose-dependent manner across all tested cell lines, including A549, HepG2, and HEK293A cells (Fig. 1A), This suggests that YAP activation by morusin is not limited to a specific cancer cell type. To explore the temporal pattern of YAP dephosphorylation, HEK293A cells were treated with morusin and analyzed for YAP phosphorylation status at various time points up to 24 h. We found that morusin induced transient dephosphorylation of YAP (Fig. 1B), with peak dephosphorylation observed at 3 h post-treatment, followed by a gradual increase in YAP S127 phosphorylation, indicating transient YAP activation (Fig. 1B). We further examined YAP transcriptional activity by measuring the mRNA levels of its downstream target genes, CTGF and CYR61 [31]. HEK293A cells treated with morusin showed a significant increase in the expression of CTGF and CYR61 in a dose-dependent manner (Fig. 1C), indicating enhanced transcriptional activity of YAP by morusin treatment. We also examined whether the transient YAP activation through S127 dephosphorylation affects its transcriptional activity by treating HEK293A cells with morusin at different time points. Time-course experiments revealed a sharp increase in CTGF mRNA levels at 1–3 h post-morusin

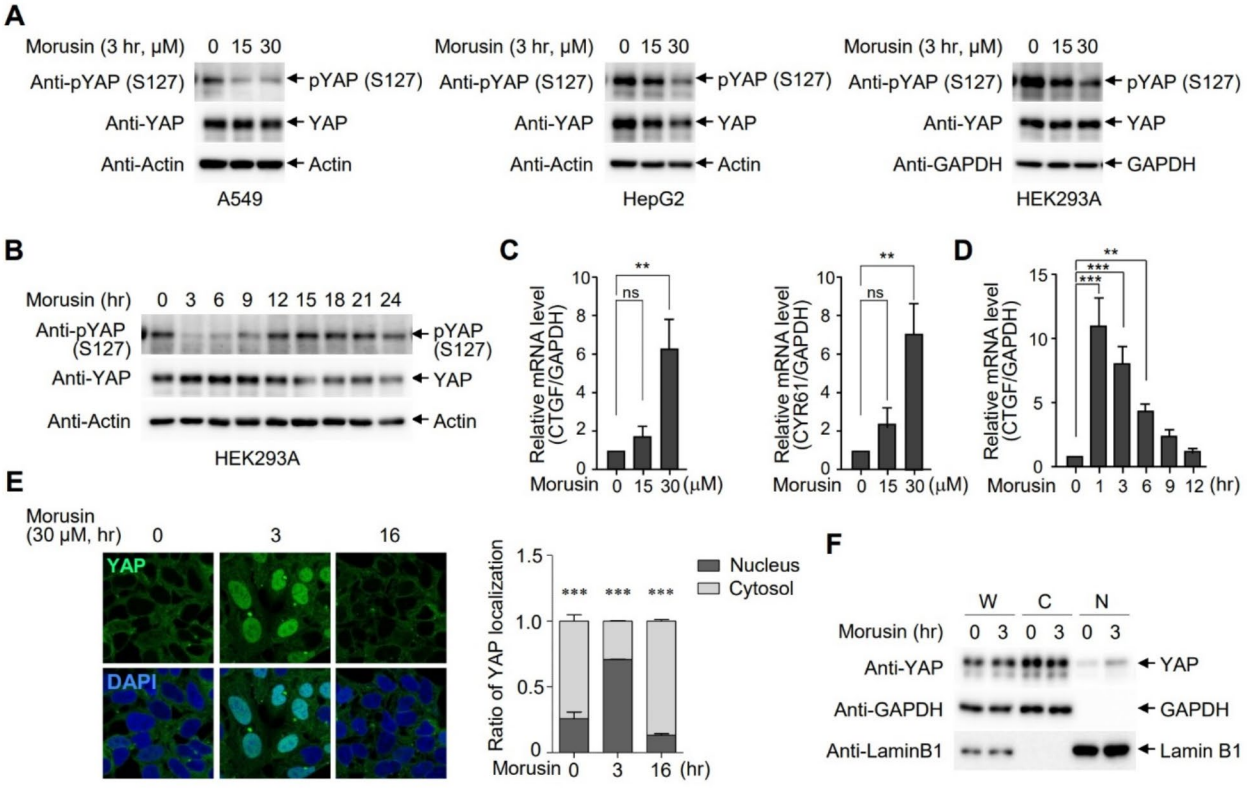

Fig. 1 Morusin induces YAP activation. (**A**) Dephosphorylation of YAP at S127 by morusin. Various cancer cell lines, including A549, HepG2, and HEK293A, were treated with either DMSO or morusin for 3 h at the indicated concentrations. The levels of YAP and its phosphorylation at S127 were determined by immunoblotting using anti-YAP and anti-pYAP(S127), respectively. (**B**) Time-course analysis of YAP activation by morusin. HEK293A cells were treated with either DMSO or morusin (30 μM) at the indicated time points. (**C**) Morusin induces transcriptional activity of YAP. HEK293A cells were treated with either DMSO or morusin for 3 h at the specified concentrations. The mRNA levels of CTGF and CYR61, which are downstream target genes of YAP, were measured to assess transcriptional activity. Statistical analysis was performed using one-way ANOVA followed by Bonferroni's multiple comparison test, where $^{**}p < 0.01$. (**D**) Transient induction of YAP transcriptional activity by morusin. HEK293A cells were treated with either DMSO or morusin (30 μM) at the indicated time points. The mRNA levels of CTGF were measured. Statistical analysis was performed using one-way ANOVA followed by Bonferroni's multiple comparison test, where $^{**}p < 0.01$, $^{***}p < 0.001$. (**E**) Nuclear localization of YAP induced by morusin. HEK293A cells were treated with either DMSO or morusin (30 μM) at the indicated time points. Endogenous YAP localization was detected via immunostaining with an anti-YAP antibody (green) and DAPI (nuclei, blue). Endogenous YAP translocated to the nucleus following morusin treatment, and nuclear YAP subsequently relocated to the cytosol at later time points. This experiment was repeated three times. The right panel illustrates the relative ratio of nuclear to cytosolic YAP localization. Statistical analysis was performed using one-way ANOVA followed by Bonferroni's multiple comparison test, where $^{***}p < 0.001$. (**F**) Morusin-induced nuclear localization of YAP. HEK293A cells were treated with either DMSO or morusin (30 μM) for 3 h, followed by nuclear and cytosolic fractionation to analyze YAP localization. GAPDH and lamin B1 were used as markers for the cytosolic and nuclear fractions, respectively. Uncropped full-length blots are presented in Supplementary Fig. 1

treatment, followed by a gradual decrease at later times (Fig. 1D). To corroborate the transient activation of YAP, we examined its nuclear translocation. Immunostaining with an anti-YAP antibody demonstrated that cytosolic YAP translocated to the nucleus immediately after morusin treatment and gradually diffused back to the cytosol at later times (Fig. 1E). Nuclear/cytosolic fractionation of HEK293A cells treated with morusin for 3 h confirmed the nuclear accumulation of YAP (Fig. 1F). Collectively, these findings demonstrate that morusin induces transient YAP activation, as evidenced by dephosphorylation at S127, nuclear localization, and increased transcriptional activity of YAP target genes, all of which reverse within 12 h post-treatment.

Morusin induces YAP activation independently of the canonical Hippo signaling pathway

To investigate the mechanism by which morusin activates YAP, we examined whether morusin influences the canonical Hippo signaling pathway. Cells treated with morusin over time were subjected to immunoblotting for key regulators of the Hippo signaling pathway. Both YAP and LATS1 exhibited similar phosphorylation patterns, with a sharp decrease in phosphorylation followed by gradual recovery post-treatment. However, morusin did not significantly affect the upstream components of the Hippo signaling pathway, including MST1/2, MOB1, and SAV1 (Fig. 2A). These results suggest that morusin activates YAP independently of the canonical

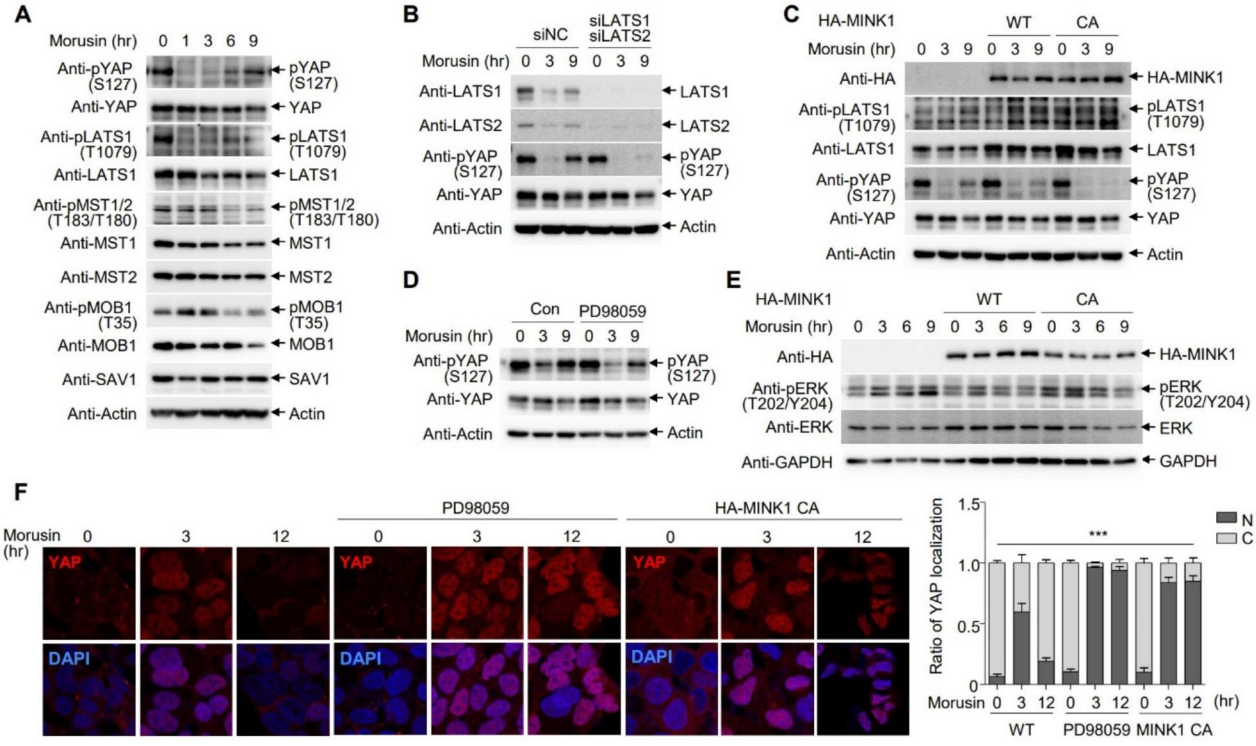

Fig. 2 Morusin induces YAP activation independently of the canonical Hippo pathway. (**A**) Transient dephosphorylation of YAP and LATS1 by morusin. HCT116 cells were treated with either DMSO or morusin (30 μM) at the indicated time points. The results demonstrate that morusin induces a transient dephosphorylation of YAP and LATS1 without affecting the upstream regulators of the Hippo pathway. (**B**) Effect of LATS1/2 depletion on morusin-induced YAP rephosphorylation. HCT116 cells were transfected with siNC or siLATS1/siLATS2 and treated with either DMSO or morusin (30 μM) at the indicated time points. The depletion of LATS1/2 alters the rephosphorylation of YAP induced by morusin. (**C**) Role of MAP4K6 (MINK1) in YAP phosphorylation independent of LATS1. HCT116 cells overexpressing either wild-type (WT) or a constitutively active form (CA) of HA-MINK1 were treated with either DMSO or morusin (30 μM) at the indicated time points. The levels of YAP, LATS, and their phosphorylations were determined by immunoblotting using the indicated antibodies. (**D**) Influence of MAPKs on YAP phosphorylation. HCT116 cells were pretreated with an MEK1 inhibitor (PD98059) to inhibit ERK1/2 activation, followed by treatment with either DMSO or morusin (30 μM) at the indicated time points. (**E**) Impact of MINK1 on ERK phosphorylation. HCT116 cells overexpressing either wild-type or a constitutively active form of HA-MINK1 were treated with either DMSO or morusin (30 μM) at the indicated time points. (**F**) Morusin-induced nuclear localization of YAP under conditions of ERK1/2 inhibition and MINK1 overexpression. HEK293A cells were pretreated with PD98059, a MEK1 inhibitor, for 1 h, and then treated with either DMSO or morusin (30 μM) at the indicated time points. Endogenous YAP localization was detected via immunostaining using an anti-YAP antibody (red) and DAPI (nuclei, blue). Morusin treatment induced the translocation of endogenous YAP to the nucleus, and nuclear YAP was retained at later time points under MEK1 inhibitor treatment and MINK1 overexpression. The right panel illustrates the relative ratio of nuclear to cytosolic YAP localization. N and C indicates nuclear and cytosol, respectively. Statistical analysis was performed using one-way ANOVA followed by Bonferroni's multiple comparison test, where $^{***}p < 0.001$. Uncropped full-length blots are presented in Supplementary Fig. 1

Hippo signaling pathway. To further explore the role of LATS1/2 in morusin-induced YAP activation, HCT116 cells depleted of LATS1/2 were treated with morusin. Depletion of LATS1/2 impaired the rephosphorylation of YAP at S127 following morusin treatment, indicating that LATS1/2 are involved in the rephosphorylation process but not in the initial YAP activation by morusin (Fig. 2B). To further investigate the upstream kinase(s) involved in YAP regulation, we examined whether MINK1 (MAP4K6), a kinase known to affect YAP phosphorylation in parallel with the MST1/2 kinases [6, 20], plays a role in YAP modulation by morusin. We generated cell lines expressing the wild-type (WT) or constitutively active (T187E) form of HA-MINK1. Cells expressing constitutively active MINK1 showed reduced YAP rephosphorylation at later times post-morusin treatment, indicating prolonged YAP activation independent of LATS1 (Fig. 2C). To confirm the independence of MINK1 regulation from LATS1, we examined the role of ERK, a downstream target of MAP4K family kinases. Treatment with an ERK inhibitor reduced YAP rephosphorylation at later times post-treatment (Fig. 2D). In cells overexpressing constitutively active MINK1, we observed reduced ERK phosphorylation at later times post-treatment (Fig. 2E), highlighting potential cross-talk between MINK1 and the ERK pathway in YAP rephosphorylation. The regulation of YAP activity by MINK1 and ERK was also assessed based on YAP localization

in the nucleus. YAP was transiently translocated to the nucleus but returned to the cytosol 12 h following morusin treatment. However, in cells treated with MEK1 inhibitor and overexpressing HA-MINK1, nuclear YAP was retained at later time points. This suggests that the inactivation of YAP's transcriptional activity through its cytosolic localization is controlled by MINK1 and ERK activities (Fig. 2F). These findings indicate that morusin activates YAP via alternative mechanisms, involving the LATS1/2, MINK1, and MAPK signaling pathways, independent of the canonical Hippo pathway.

Depletion of YAP/TAZ affects morusin-induced stress granule formation

Stress granule formation provides resistance against morusin-induced apoptosis [42]. Since stress granule formation peaks at 3 h post-morusin treatment, coinciding with YAP activation, we investigated whether YAP/TAZ contribute to stress granule formation and confer resistance to morusin-induced apoptosis. We assessed the role of YAP/TAZ in morusin-induced stress granule formation by depleting A549 cells of YAP/TAZ and treating them with morusin. Stress granule formation, evaluated by detecting endogenous G3BP1 puncta through immunostaining, was significantly diminished in YAP/TAZ-depleted cells, as indicated by the reduced presence of G3BP1 puncta (Fig. 3A). Stress granules formed 30 min post-morusin treatment, peaked at 3 h, and gradually disassembled over time. However, YAP/TAZ depletion resulted in a 70% reduction in stress granule formation across all time points (Fig. 3B and C). These results indicate that YAP/TAZ are crucial for morusin-induced stress granule formation.

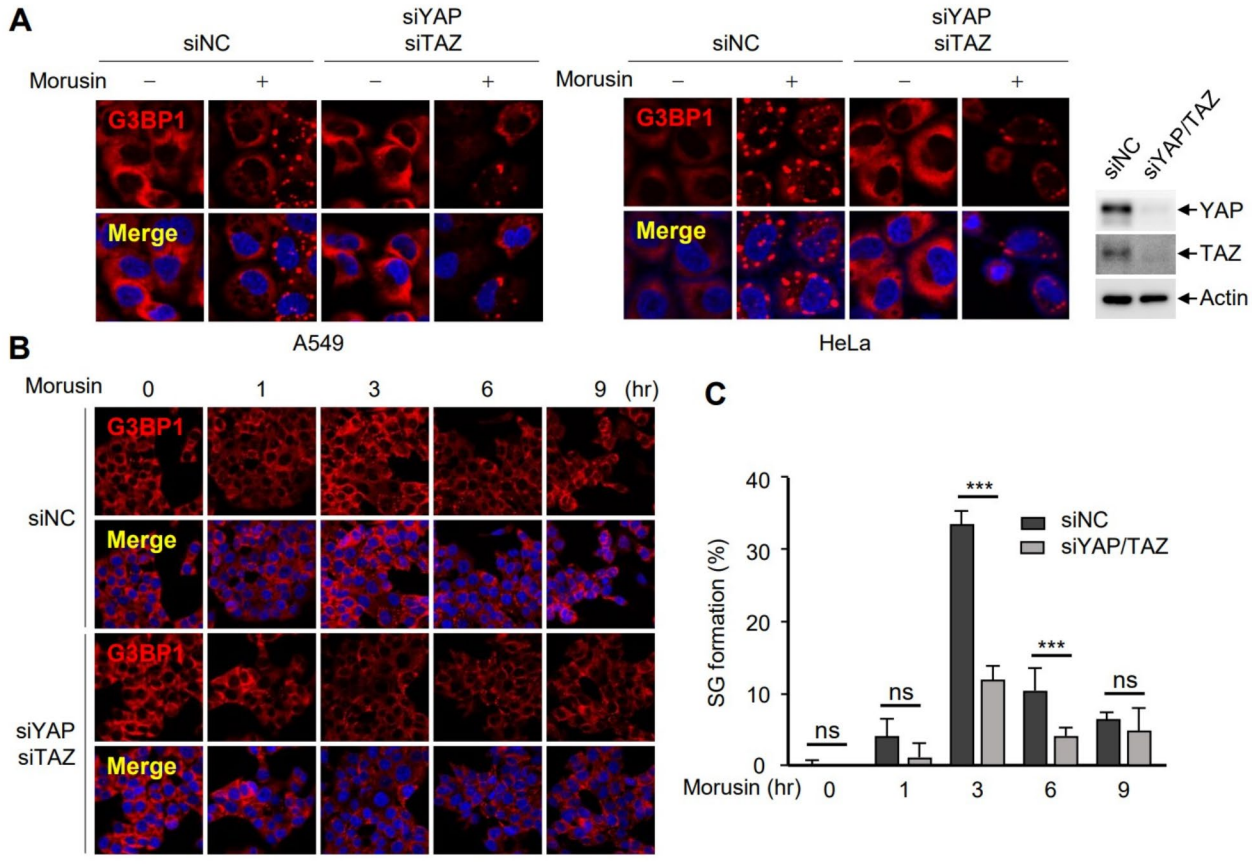

Fig. 3 Depletion of YAP/TAZ affects morusin-induced stress granule formation. (**A**) Reduced stress granule formation due to YAP/TAZ depletion. A549 and HeLa cells were transfected with either siNC or siYAP/siTAZ and treated with either DMSO or morusin (30 μM) for 3 h. Endogenous G3BP1 puncta were detected using immunostaining with an anti-G3BP1 antibody. Depletion of YAP and TAZ was confirmed by immunoblotting with anti-YAP/TAZ antibody. (**B**) Time-dependent effect of YAP/TAZ depletion on stress granule formation. HCT116 cells were transfected with either siNC or siYAP/siTAZ and treated with either DMSO or morusin (30 μM) at the indicated time points. Endogenous G3BP1 puncta were detected using immunostaining with an anti-G3BP1 antibody. (**C**) Quantitation of cells with G3BP1 puncta. The percentage of cells exhibiting G3BP1 puncta were quantified in three different arbitrary areas and is presented in the graph. Data are shown as the mean ± SEM. Statistical analysis was performed by one-way analysis of variance (ANOVA) followed by Bonferroni's multiple comparison test (***$p < 0.001$ compared to the indicated points; $n = 3$)

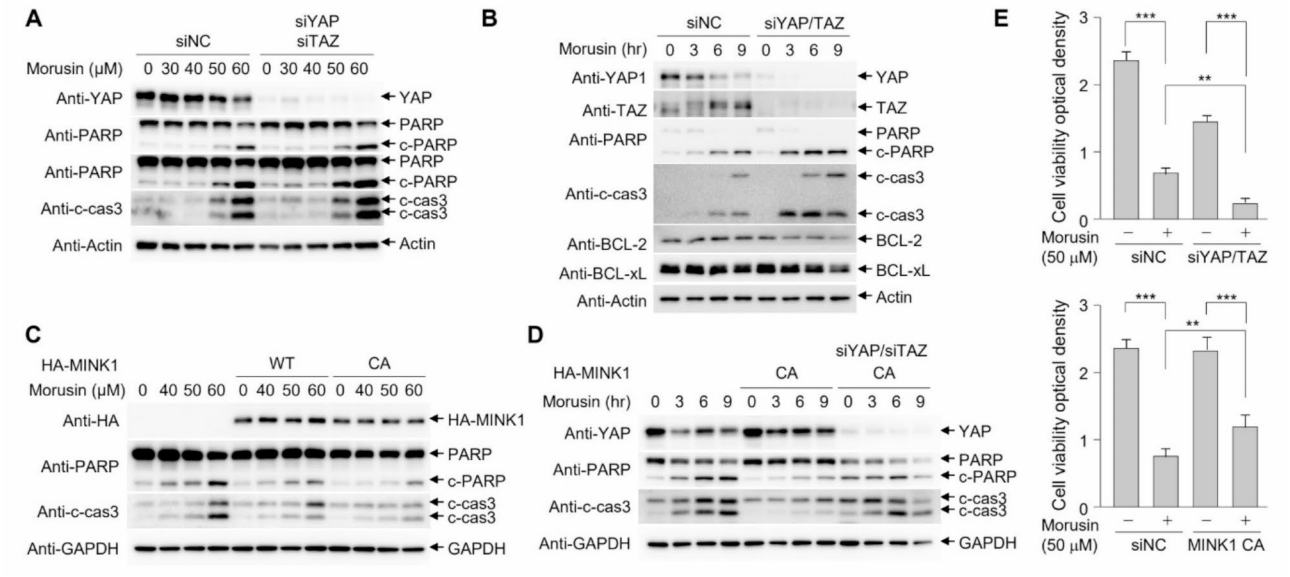

Fig. 4 Depletion of YAP/TAZ affects morusin-induced apoptosis. (**A**) Enhanced morusin-induced apoptosis due to YAP/TAZ depletion in a dose-dependent manner. HEK293A cells were transfected with either siNC or siYAP/siTAZ and treated with either DMSO or morusin for 6 h at the indicated concentrations. (**B**) Enhanced morusin-induced apoptosis due to YAP/TAZ depletion in a time-dependent manner. HeLa cells were transfected with either siNC or siYAP/siTAZ and treated with either DMSO or morusin (50 μM) at the indicated time points. (**C**) MINK1 modulates morusin-induced apoptosis in a dose-dependent manner. HCT116 cells overexpressing either wild-type (WT) or a constitutively active form (CA) of HA-MINK1 were treated with either DMSO or morusin for 6 h at the indicated concentrations. (**D**) MINK1 modulates morusin-induced apoptosis in a time-dependent manner. HCT116 cells overexpressing either wild-type, a constitutively active form of HA-MINK1 or YAP/TAZ-depleted HA-MINK1 CA were treated with either DMSO or morusin (50 μM) at the indicated time points. (**E**) Determination of cell survival using the MTT assay. HeLa cells were depleted of YAP/TAZ or overexpressed with MINK1 CA and treated with either DMSO or morusin for 4 h at the indicated concentrations. Cell viability was assessed by measuring the optical density of the MTT-formazan product. Statistical analysis was performed using one-way ANOVA followed by Bonferroni's multiple comparison test, where $^{***}p < 0.001$, $^{**}p < 0.01$. Uncropped full-length blots are presented in Supplementary Fig. 1

YAP/TAZ confer resistance to morusin-induced apoptosis

Given that YAP/TAZ are required for morusin-induced stress granule formation, which affects the induction of apoptosis, we investigated the effects of YAP/TAZ on morusin-induced apoptosis. Treatment of HEK293A cells with increasing amounts of morusin for 6 h led to apoptosis, as evidenced by the dose-dependent cleavage of PARP and caspase-3. However, YAP/TAZ depletion increased the levels of cleaved PARP and caspase-3, indicating accelerated apoptosis (Fig. 4A). When HeLa cells were exposed to 50 μM morusin over time, cleavage of PARP and caspase-3 occurred earlier in YAP/TAZ-depleted cells, suggesting that YAP/TAZ confer resistance to apoptosis. Consistently, the levels of Bcl-2 and Bcl-xL were reduced in YAP/TAZ-depleted cells in a time-dependent manner following morusin treatment, but not in mock-depleted cells (Fig. 4B). We also examined the impact of MINK1 on morusin-induced apoptosis. Expression of constitutively active MINK1 abrogated YAP rephosphorylation at later times post-morusin treatment, suggesting prolonged YAP activation (Fig. 2C). To determine whether MINK1-mediated YAP activation affects morusin-induced apoptosis, HCT116 cells expressing wild-type or a constitutively active (CA) form of HA-MINK1 were treated with increasing amounts of morusin. Immunoblotting showed reduced PARP and caspase-3 cleavage in HA-MINK1 CA-expressing cells (Fig. 4C). However, MINK1-mediated suppression of apoptosis was reversed by YAP/TAZ depletion (Fig. 4D), indicating that MINK1 inhibits apoptosis through prolonged activation of YAP/TAZ. Consistently, cell viability decreased upon morusin treatment in YAP/TAZ-depleted cells but increased in cells expressing MINK1 CA (Fig. 4E). Taken together, we propose a novel model in which YAP/TAZ orchestrate a protective role against morusin-induced apoptosis.

Discussion

Tumor cells frequently develop sophisticated strategies to evade cell death induced by anti-cancer drugs, leading to limited clinical drug efficacy, tumor progression, and recurrence. These strategies often involve enhanced drug efflux, epithelial-mesenchymal transition, persistence of cancer stem cells, downregulation of apoptosis, and drug-resistant mutations [44]. This study investigates the regulatory mechanisms that control YAP activity in tumor cells following morusin treatment. A key finding is that the transient YAP activation enhances stress granule (SG) formation, thereby contributing to resistance against morusin-induced apoptosis. The Hippo pathway

plays a crucial role in regulating cell proliferation, apoptosis, and stem cell self-renewal [45]. It primarily involves a kinase cascade and transcriptional coactivators, such as MST1/2, LATS1/2, and YAP/TAZ, in its canonical pathway. In noncanonical pathways, however, YAP and TAZ are regulated by various other proteins and signaling mechanisms. These include direct regulators of YAP phosphorylation and activity, such as AMPK and NDR1/2 [18, 46], as well as indirect regulators, such as Rho GTPase [47], E3 ubiquitin ligases including PARK2 [48], and AMPK-derived metabolic regulators that target LATS1/2 kinase [18]. Moreover, MAP4K family kinases have been identified to regulate YAP phosphorylation in parallel with the MST1/2 kinases [20]. This study highlights the dual role of MAP4K4 family kinases, which are known to act as physiological LATS-activating kinases. Notably, MAP4K4/6/7 kinases regulate LATS1/2 in parallel with MST1/2 and influence YAP regulation by cell density. However, the current findings reveal more intricate interactions between YAP upstream kinases depending on the cellular context. Specifically, the study demonstrates that morusin-induced dephosphorylation of YAP is unaffected by LATS1/2 depletion or MINK1 (MAP4K6) overexpression during the early phase of YAP activation. In contrast, the rephosphorylation of YAP, corresponding to YAP inactivation observed 9 h post-morusin treatment, is inhibited by both LATS1/2 depletion and MINK1 overexpression (Fig. 2B and C). These results suggest that MINK1 does not function as an upstream kinase for LATS1/2 in the context of phosphorylation-mediated YAP inactivation during the later stages of morusin treatment, implicating a different regulatory mechanism in YAP rephosphorylation (Fig. 2C). The negative feedback loop between the LATS1/2 kinases and YAP is crucial for maintaining cellular homeostasis by ensuring precise control of the amplitude and duration of YAP activation [49]. When YAP is activated and translocates to the nucleus, it induces the expression of LATS1/2 and AMOTL2 at the transcriptional level, leading to YAP phosphorylation and inactivation, thereby preventing excessive activity that could lead to uncontrolled cell proliferation [49]. The findings in this study support the notion that this feedback mechanism remains functional during the rephosphorylation phase post-morusin treatment, as indicated by the inhibition of YAP rephosphorylation upon LATS1/2 depletion (Fig. 2B). Furthermore, the dual functionality of MINK1 is highlighted in its role in maintaining YAP activation. MINK1 does not act as an upstream kinase for LATS1/2 during the initial dephosphorylation phase, as YAP S127 dephosphorylation occurred even under conditions of MINK1 CA overexpression and LATS1/2 activation, indicating that YAP activation predominates under conditions of LATS1/2 activation. On the other hand, MINK1 appears to participate in the negative feedback loop governing YAP rephosphorylation at later stages, where YAP activity was maintained by MINK1 overexpression (Fig. 2C). This underscores the complexity of MINK1 involvement in YAP signaling pathways, suggesting that MAP4K family kinases can modulate YAP activity through both LATS1/2-dependent and -independent mechanisms, depending on the specific cellular signaling context. In addition to its role in YAP regulation, MINK1 modulates ERK activity, contributing to the broader MAP kinase signaling network. The data indicate that MINK1 can influence ERK phosphorylation, thereby affecting downstream cellular processes such as YAP-mediated apoptosis resistance (Fig. 4D). This dual functionality underscores the versatile role of MAP4K family kinases in the Hippo signaling pathway. Morusin induces transient activation of YAP, during which YAP translocates to the nucleus and subsequently returns to the cytosol before triggering apoptosis. However, under conditions of ERK inhibition and MINK1 overexpression, the restoration of cytosolic YAP localization was inhibited, leading to the sustained presence of transcriptionally active nuclear YAP. ERK1/2 predominantly localizes in the cytosol and does not participate in YAP's nuclear entry during the early stage of morusin treatment. Given the differential compartmentalization of cytosolic ERK1/2 and nuclear YAP, it is unlikely that ERK1/2 directly controls YAP localization through phosphorylation. It is well known that YAP activation is mediated by cytoskeletal tension induced by mechanical stress, which is regulated by Rho-GTPase activity [50, 51]. Similarly, ERK1/2 may indirectly regulate YAP/TAZ activity through its effects on cytoskeletal organization by promoting actin polymerization and stabilizing microtubules, both of which serve as upstream signals for YAP/TAZ nuclear translocation.

The depletion of YAP/TAZ in cells results in enhanced apoptosis and impaired SG formation, highlighting the multifaceted roles of these transcriptional co-activators in cell survival mechanisms. YAP/TAZ may inhibit apoptosis through both direct and indirect mechanisms. It is known that YAP/TAZ inhibit apoptosis by promoting the transcription of anti-apoptotic genes, such as BIRC5 (Survivin) and BCL2 [52, 53], which are crucial for cell survival. By ensuring the expression of these genes, YAP/TAZ help maintain cellular integrity and prevent morusin-induced apoptosis. Indirectly, YAP/TAZ play a significant role in the formation of SGs, which are crucial for the cellular stress response to morusin [42]. SGs sequester translating mRNA-protein complexes, thereby delaying translation and preventing the activation of apoptotic pathways by sequestering pro-apoptotic proteins such as RACK1 [42]. In YAP/TAZ-depleted cells, SG formation was markedly impaired during the phases

of SG formation and disassembly, which may enhance the apoptotic response through the release of apoptotic proteins. YAP activity and stability are regulated by various signaling inputs, such as cell-cell contact, mechanotransduction from the cell surface, and cytoskeletal structure governed by Rho GTPase. Moreover, YAP not only responds to upstream signals such as cytoskeletal organization and cell adhesion but also plays an active role in regulating cytoskeletal organization [54]. YAP/TAZ are known to regulate actin cytoskeleton organization through the transcriptional upregulation of RhoA suppressors, resulting in reduced cytoskeletal rigidity and the promotion of a metastatic phenotype [55]. Microtubules, which are components of the three-dimensional cytoskeleton, mediate force transmission. YAP mediates microtubule stabilization to promote cartilage formation and type II collagen expression [56]. YAP/TAZ act as signaling hubs to perceive various mechanical signaling inputs and convert them into cytoskeletal reorganization, facilitating cell migration and cell polarity during development and differentiation [54]. SGs are transiently induced dynamic structures, through a series of events including the formation of SG core particles, coalescence of pre-formed granules, transport to the perinuclear region, and disassembly. Microtubules are known to function in SG coalescence and disassembly through direct association with SGs [57]. In YAP/TAZ-depleted cells, both the number and size of SGs were markedly reduced (Fig. 3A), potentially due to the loss of SG coalescence caused by a reduced microtubule network. Thus, the interplay between YAP/TAZ and cytoskeletal components might influence SG dynamics through microtubule-mediated transport of SGs [58]. Disruption of the cytoskeletal framework due to YAP/TAZ depletion can hinder SG assembly, further compromising cell survival by facilitating apoptosis under stress conditions. Collectively, YAP/TAZ protect cells from apoptosis through both direct transcriptional activation of anti-apoptotic genes and the indirect promotion of SG formation. The impairment of SGs in YAP/TAZ-depleted cells leads to enhanced apoptosis, illustrating the critical role of SGs in YAP/TAZ-mediated buffering of cellular stress and maintenance of cell viability.

Conclusions

This study demonstrates that morusin transiently induces YAP activation, leading to its nuclear localization by S127 dephosphorylation and increased transcriptional activity of target genes, independent of the canonical Hippo signaling pathway. This activation involves alternative regulatory mechanisms, including the LATS1/2, MINK1, and MAPK signaling pathways. Additionally, we found that YAP/TAZ play a critical role in stress granule formation, conferring resistance to morusin-induced apoptosis. The depletion of YAP/TAZ significantly impairs stress granule formation and enhances apoptosis, suggesting that targeting YAP/TAZ may enhance the therapeutic efficacy of morusin in cancer treatment. Since several YAP/TAZ inhibitors are currently in development and phase I clinical trials [59], a combinatorial treatment of morusin with YAP/TAZ inhibitors holds promise for enhancing therapeutic outcomes. These findings provide new insights into the molecular mechanisms underlying the anti-cancer effects of morusin and propose potential strategies for overcoming resistance to apoptosis in cancer cells.

Supplementary Information

The online version contains supplementary material available at https://doi.org/10.1186/s12860-025-00531-1.

Supplementary Material 1

Acknowledgements
The authors are very grateful to Min Sung Choi for critical reading of manuscript.

Author contributions
Conceptualization, H.Y.L., S.W.C., and C.Y.C.; methodology, S.W.C.; investigation, H.S.C.; data curation, K.T.; writing–original draft preparation, H.Y.L. and S.W.C.; writing–review and editing, S.W.C., H.Y.L., H.S.C. and C.Y.C.; supervision, C.Y.C.

Funding
This work was supported by the National Research Foundation of Korea (grant 2021-R1A2C1011197 to C.Y.C.) funded by the Korea Ministry of Science and ICT.

Data availability
The data are available from the corresponding author upon reasonable request.

Declarations

Ethics approval and consent to participate
Not applicable.

Consent for publication
Not applicable.

Competing interests
The authors declare no competing interests.

Received: 26 August 2024 / Accepted: 14 January 2025
Published online: 20 January 2025

References

1. Ma S, Meng Z, Chen R, Guan KL. The Hippo Pathway: Biology and Pathophysiology. Annu Rev Biochem. 2019;88:577–604.
2. Fu M, Hu Y, Lan T, Guan KL, Luo T, Luo M. The Hippo signalling pathway and its implications in human health and diseases. Signal Transduct Target Ther. 2022;7(1):376.
3. Cunningham R, Hansen CG. The Hippo pathway in cancer: YAP/TAZ and TEAD as therapeutic targets in cancer. Clin Sci (Lond). 2022;136(3):197–222.
4. Driskill JH, Pan D. The Hippo Pathway in Liver Homeostasis and Pathophysiology. Annu Rev Pathol. 2021;16:299–322.
5. Wu S, Huang J, Dong J, Pan D. Hippo encodes a Ste-20 family protein kinase that restricts cell proliferation and promotes apoptosis in conjunction with salvador and warts. Cell. 2003;114(4):445–56.

6. Meng Z, Moroishi T, Guan KL. Mechanisms of Hippo pathway regulation. Genes Dev. 2016;30(1):1–17.
7. Dey A, Varelas X, Guan KL. Targeting the Hippo pathway in cancer, fibrosis, wound healing and regenerative medicine. Nat Rev Drug Discov. 2020;19(7):480–94.
8. Harvey KF, Zhang X, Thomas DM. The Hippo pathway and human cancer. Nat Rev Cancer. 2013;13(4):246–57.
9. He M, Zhou Z, Shah AA, Hong Y, Chen Q, Wan Y. New insights into posttranslational modifications of Hippo pathway in carcinogenesis and therapeutics. Cell Div. 2016;11:4.
10. Liu H, Du S, Lei T, Wang H, He X, Tong R, et al. Multifaceted regulation and functions of YAP/TAZ in tumors (review). Oncol Rep. 2018;40(1):16–28.
11. Zhao B, Li L, Tumaneng K, Wang CY, Guan KL. A coordinated phosphorylation by lats and CK1 regulates YAP stability through SCF(beta-TRCP). Genes Dev. 2010;24(1):72–85.
12. Zhao B, Ye X, Yu J, Li L, Li W, Li S, et al. TEAD mediates YAP-dependent gene induction and growth control. Genes Dev. 2008;22(14):1962–71.
13. Lüönd F, Pirkl M, Hisano M, Prestigiacomo V, Kalathur RK, Beerenwinkel N et al. Hierarchy of TGFβ/SMAD, Hippo/YAP/TAZ, and Wnt/β-catenin signaling in melanoma phenotype switching. Life Sci Alliance. 2022;5(2).
14. Passaniti A, Brusgard JL, Qiao Y, Sudol M, Finch-Edmondson M. Roles of RUNX in Hippo Pathway Signaling. Adv Exp Med Biol. 2017;962:435–48.
15. Azzolin L, Panciera T, Soligo S, Enzo E, Bicciato S, Dupont S, et al. YAP/TAZ incorporation in the β-catenin destruction complex orchestrates the wnt response. Cell. 2014;158(1):157–70.
16. Gao Y, Yang Y, Yuan F, Huang J, Xu W, Mao B, et al. TNFα-YAP/p65-HK2 axis mediates breast cancer cell migration. Oncogenesis. 2017;6(9):e383.
17. Wang S, Xie F, Chu F, Zhang Z, Yang B, Dai T, et al. YAP antagonizes innate antiviral immunity and is targeted for lysosomal degradation through IKKε-mediated phosphorylation. Nat Immunol. 2017;18(7):733–43.
18. Mo JS, Meng Z, Kim YC, Park HW, Hansen CG, Kim S, et al. Cellular energy stress induces AMPK-mediated regulation of YAP and the Hippo pathway. Nat Cell Biol. 2015;17(4):500–10.
19. Wang W, Xiao ZD, Li X, Aziz KE, Gan B, Johnson RL, et al. AMPK modulates Hippo pathway activity to regulate energy homeostasis. Nat Cell Biol. 2015;17(4):490–9.
20. Meng Z, Moroishi T, Mottier-Pavie V, Plouffe SW, Hansen CG, Hong AW, et al. MAP4K family kinases act in parallel to MST1/2 to activate LATS1/2 in the Hippo pathway. Nat Commun. 2015;6:8357.
21. Das S, Khan TH, Sarkar D. Comprehensive Review on the Effect of Stem cells in Cancer Progression. Curr Tissue Microenvironment Rep. 2024;5(2):39–59.
22. Wang Y, Yu A, Yu FX. The Hippo pathway in tissue homeostasis and regeneration. Protein Cell. 2017;8(5):349–59.
23. Miao J, Hsu PC, Yang YL, Xu Z, Dai Y, Wang Y, et al. YAP regulates PD-L1 expression in human NSCLC cells. Oncotarget. 2017;8(70):114576–87.
24. Tang D, Xu H, Du X. The role of non-canonical Hippo pathway in regulating immune homeostasis. Eur J Med Res. 2023;28(1):498.
25. Mia MM, Singh MK. Emerging roles of the Hippo signaling pathway in modulating immune response and inflammation-driven tissue repair and remodeling. Febs j. 2022;289(14):4061–81.
26. Khan TH, Srivastava N, Srivastava A, Sareen A, Mathur RK, Chande AG, et al. SHP-1 plays a crucial role in CD40 signaling reciprocity. J Immunol. 2014;193(7):3644–53.
27. Zhang X, Kiapour N, Kapoor S, Khan T, Thamilarasan M, Tao Y, et al. IL-11 induces encephalitogenic Th17 cells in multiple sclerosis and experimental autoimmune encephalomyelitis. J Immunol. 2019;203(5):1142–50.
28. Seyedsadr M, Wang Y, Elzoheiry M, Shree Gopal S, Jang S, Duran G, et al. IL-11 induces NLRP3 inflammasome activation in monocytes and inflammatory cell migration to the central nervous system. Proc Natl Acad Sci U S A. 2023;120(26):e2221007120.
29. Moya IM, Halder G. Hippo-YAP/TAZ signalling in organ regeneration and regenerative medicine. Nat Rev Mol Cell Biol. 2019;20(4):211–26.
30. Panek-Krzyśko A, Stompor-Gorący M. The Pro-health benefits of Morusin Administration-An Update Review. Nutrients. 2021;13(9).
31. Choi DW, Cho SW, Lee SG, Choi CY. The Beneficial effects of Morusin, an Isoprene Flavonoid isolated from the Root Bark of Morus. Int J Mol Sci. 2020;21(18):6541.
32. Jia Y, He W, Zhang H, He L, Wang Y, Zhang T, et al. Morusin ameliorates IL-1β-Induced Chondrocyte inflammation and osteoarthritis via NF-κB Signal Pathway. Drug Des Devel Ther. 2020;14:1227–40.
33. Lim SL, Park SY, Kang S, Park D, Kim SH, Um JY, et al. Morusin induces cell death through inactivating STAT3 signaling in prostate cancer cells. Am J Cancer Res. 2015;5(1):289–99.
34. Liu W, Ji Y, Wang F, Li C, Shi S, Liu R, et al. Morusin shows potent antitumor activity for melanoma through apoptosis induction and proliferation inhibition. BMC Cancer. 2023;23(1):602.
35. Wang J, Liu X, Zheng H, Liu Q, Zhang H, Wang X, et al. Morusin induces apoptosis and autophagy via JNK, ERK and PI3K/Akt signaling in human lung carcinoma cells. Chem Biol Interact. 2020;331:109279.
36. Xue J, Li R, Zhao X, Ma C, Lv X, Liu L, et al. Morusin induces paraptosis-like cell death through mitochondrial calcium overload and dysfunction in epithelial ovarian cancer. Chem Biol Interact. 2018;283:59–74.
37. Yang C, Luo J, Luo X, Jia W, Fang Z, Yi S, et al. Morusin exerts anti-cancer activity in renal cell carcinoma by disturbing MAPK signaling pathways. Ann Transl Med. 2020;8(6):327.
38. Martins BA, Sande D, Solares MD, Takahashi JA. Antioxidant role of morusin and mulberrofuran B in ethanol extract of Morus alba roots. Nat Prod Res. 2021;35(24):5993–6.
39. Pang D, Liao S, Wang W, Mu L, Li E, Shen W, et al. Destruction of the cell membrane and inhibition of cell phosphatidic acid biosynthesis in Staphylococcus aureus: an explanation for the antibacterial mechanism of morusin. Food Funct. 2019;10(10):6438–46.
40. Kim C, Kim JH, Oh EY, Nam D, Lee SG, Lee J, et al. Blockage of STAT3 signaling pathway by Morusin induces apoptosis and inhibits Invasion in Human pancreatic tumor cells. Pancreas. 2016;45(3):409–19.
41. Cho SW, Na W, Choi M, Kang SJ, Lee SG, Choi CY. Autophagy inhibits cell death induced by the anti-cancer drug morusin. Am J Cancer Res. 2017;7(3):518–30.
42. Park YJ, Choi DW, Cho SW, Han J, Yang S, Choi CY. Stress granule formation attenuates RACK1-Mediated apoptotic cell Death Induced by Morusin. Int J Mol Sci. 2020;21(15).
43. Zhou W, Lim A, Edderkaoui M, Osipov A, Wu H, Wang Q, et al. Role of YAP Signaling in Regulation of programmed cell death and Drug Resistance in Cancer. Int J Biol Sci. 2024;20(1):15–28.
44. Aleksakhina SN, Kashyap A, Imyanitov EN. Mechanisms of acquired tumor drug resistance. Biochim Biophys Acta Rev Cancer. 2019;1872(2):188310.
45. Driskill JH, Pan D. Control of stem cell renewal and fate by YAP and TAZ. Nat Rev Mol Cell Biol. 2023;24(12):895–911.
46. Hergovich A. The roles of NDR Protein Kinases in Hippo Signalling. Genes (Basel). 2016;7(5).
47. Luo J, Yu FX. GPCR-Hippo Signaling in Cancer. Cells. 2019;8(5).
48. Zhou X, Li Y, Wang W, Wang S, Hou J, Zhang A, et al. Regulation of Hippo/YAP signaling and Esophageal Squamous Carcinoma progression by an E3 ubiquitin ligase PARK2. Theranostics. 2020;10(21):9443–57.
49. Dai X, Liu H, Shen S, Guo X, Yan H, Ji X, et al. YAP activates the Hippo pathway in a negative feedback loop. Cell Res. 2015;25(10):1175–8.
50. Elosegui-Artola A, Andreu I, Beedle AEM, Lezamiz A, Uroz M, Kosmalska AJ, et al. Force triggers YAP Nuclear Entry by regulating transport across Nuclear pores. Cell. 2017;171(6):1397–e41014.
51. Cai X, Wang KC, Meng Z. Mechanoregulation of YAP and TAZ in Cellular Homeostasis and Disease Progression. Front Cell Dev Biol. 2021;9:673599.
52. Li X, Lin YY, Tan JY, Liu KL, Shen XL, Hu YJ, et al. Lappaol F, an anticancer agent, inhibits YAP via transcriptional and post-translational regulation. Pharm Biol. 2021;59(1):619–28.
53. Kumar A, BharathwajChetty B, Manickasamy MK, Unnikrishnan J, Alqahtani MS, Abbas M, et al. Natural compounds targeting YAP/TAZ axis in cancer: current state of art and challenges. Pharmacol Res. 2024;203:107167.
54. Totaro A, Panciera T, Piccolo S. YAP/TAZ upstream signals and downstream responses. Nat Cell Biol. 2018;20(8):888–99.
55. Qiao Y, Chen J, Lim YB, Finch-Edmondson ML, Seshachalam VP, Qin L, et al. YAP regulates actin dynamics through ARHGAP29 and promotes metastasis. Cell Rep. 2017;19(8):1495–502.
56. Zhang X, Shu S, Feng Z, Qiu Y, Bao H, Zhu Z. Microtubule stabilization promotes the synthesis of type 2 collagen in nucleus pulposus cell by activating hippo-yap pathway. Front Pharmacol. 2023;14:1102318.
57. Bartoli KM, Bishop DL, Saunders WS. The role of molecular microtubule motors and the microtubule cytoskeleton in stress granule dynamics. Int J Cell Biol. 2011;2011:939848.

58. Halder G, Dupont S, Piccolo S. Transduction of mechanical and cytoskeletal cues by YAP and TAZ. Nat Rev Mol Cell Biol. 2012;13(9):591–600.
59. Kumar R, Hong W. Hippo Signaling at the hallmarks of Cancer and Drug Resistance. Cells. 2024;13(7).

Publisher's note